

# Collision Resolution with Deep Reinforcement Learning for Random Access in Machine-Type Communication

Muhammad Awais Jadoon, Adriano Pastore, and Monica Navarro,  
Centre Tecnològic Telecomunicacions Catalunya (CTTC)/CERCA, Castelldefels, Spain  
Email: {mjadoon, apastore, mnavarro}@cttc.es

**Abstract**—Grant-free random access (RA) techniques are suitable for machine-type communication (MTC) networks but they need to be adaptive to the MTC traffic, which is different from the human-type communication. Conventional RA protocols such as exponential backoff (EB) schemes for slotted-ALOHA suffer from a high number of collisions and they are not directly applicable to the MTC traffic models. In this work, we propose to use multi-agent deep Q-network (DQN) with parameter sharing to find a single policy applied to all machine-type devices (MTDs) in the network to resolve collisions. Moreover, we consider binary broadcast feedback common to all devices to reduce signalling overhead. We compare the performance of our proposed DQN-RA scheme with EB schemes for up to 500 MTDs and show that the proposed scheme outperforms EB policies and provides a better balance between throughput, delay and collision rate.

**Index Terms**—Random access, multi-agent DRL, MTC, packet delay, collision resolution.

## I. INTRODUCTION

The MTC paradigm poses multiple challenges in terms of multiple access due to different its traffic characteristics as compared to the conventional human-type communication (HTC). For MTC, a small area is expected to have a thousand number of low-power low-complexity MTDs with different sleep cycles and having short packet length [1]. To manage massive access in such a scenario, if on the one hand grant-based scheduling techniques incur a huge signaling overhead, on the other hand, uncoordinated grant-free RA schemes that are more favorable for MTC traffic such as EB schemes for slotted ALOHA, suffer from high number of collisions. In uncoordinated RA, each device selects a random physical resource and transmit its data to the receiver. A huge amount of work on EB schemes in the literature exists but their performance is highly dependent on traffic arrival models and due to the complexity of the process involved, the analytical approaches provide different solutions for varying underlying assumptions [2].

In the recent state-of-the-art works, reinforcement learning (RL)-based schemes for multiple access are popular due to their ability to adapt to different traffic models. Several works including [3]–[8] but not limited to, have proposed deep reinforcement learning (DRL)-based RA solutions in wireless networks. However, their solutions are not tailored for MTC networks and most of these works consider all devices to be active and always having a packet in their buffer. This

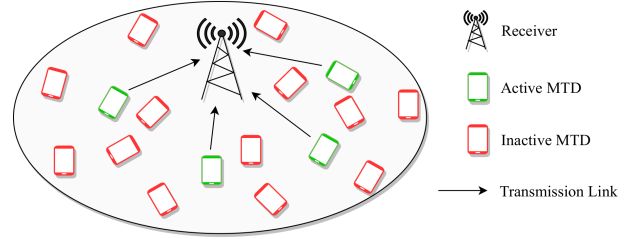


Fig. 1. An MTC network with active and inactive MTDs and a common receiver

is not the case for MTC networks where due to the varying sleep cycles of battery-constrained MTDs, they can become active/inactive in the network randomly. Moreover, for multi-agent DRL, these schemes do not provide insights into whether their proposed schemes are scalable to a higher number of users in the network or not, when a single resource (channel) is shared among users. The methods proposed in [9] still incur a high signaling overhead for scheduling and also for cooperation among devices.

In our previous work [10], we proposed DQN-based RA algorithm a (DQN-RA) that adapts to different packet traffic arrival rates that follow independent Poisson processes and it provides better performance terms of throughput and fairness as compared to the EB schemes. Our proposed DQN-RA scheme is not dependent on any specific arrival process and therefore, any random arrival process can be employed. In this work we extend our model to a higher number of devices and show how MTDs cooperatively resolve collisions and empty their packet buffers within  $K$  time slots, where  $K$  is variable and it is dependent on the total number of MTDs in the network and the traffic arrival rate. Moreover, we consider that MTDs can become active/inactive in the network and even new devices can join the network. To reduce the signaling, we consider binary broadcast feedback that informs all the active devices whether or not a collision has occurred at each time slot instead of the feedback sent to each device individually.

## II. SYSTEM MODEL AND PROBLEM FORMULATION

We consider a synchronous time-slotted MTC network as shown in Fig. 1 with a set  $\mathcal{N} = \{1, \dots, N\}$  of MTDs and an error-free broadcast channel. The physical time is divided

into discrete slots, each of duration normalized to 1 and the slot index is  $k \in \mathbb{N}$ . We assume  $\mathcal{N}_a(k) \subseteq \mathcal{N}$  as the set of active MTDs at time slot  $k$ . The packet arrival follows a Poisson process for each device  $n$  with average arrival rate  $\lambda_n$ . We assume the device  $n$  to be active when it has a packet in its buffer  $B_n(k)$  at time slot  $k$ , otherwise it is assumed to be inactive, i.e.,  $B_n(k) \in \{0, 1\}$ . We assume that each device  $n$  can only store a maximum of one packet in its buffer. Furthermore, we assume that at each time slot  $k$ , an MTD can transmit only one packet. MTDs are assumed to be slot-synchronized. After transmitting the packet, the MTD goes back to inactive/sleep mode. At each time slot  $k$ , if  $B_n(k) = 1$ , the device  $n$  takes an action  $A_n(k) \in \mathcal{A} = \{0, 1\}$ , where  $A_n(k) = 0$  corresponds to the event when the device  $n$  chooses to not transmit and  $A_n(k) = 1$  corresponds to the event when device  $n$  transmits a packet on the channel. Furthermore, for the inactive devices, we let  $A_n(k) = 0$ . After taking an action, we assume that for each time slot  $k$ , the receiver sends a broadcast feedback signal  $F(k)$  to all the active devices. We define

$$F(k) = \begin{cases} 0 & \text{if there is a collision} \\ 1 & \text{otherwise.} \end{cases} \quad (1)$$

The feedback signal  $F(k)$  and the action  $A_n(k)$  of each MTD can be used to calculate the *collision* event  $C_n(k) \in \{0, 1\}$  and the *success* event  $G_n(k) \in \{0, 1\}$  for each device  $n$ , i.e.,  $g : (F(k), A_n(k)) \mapsto (C_n(k), G_n(k))$ . These events are locally computed by each MTD and define the success event  $G_n(k)$  when a packet has been successfully transmitted by the device  $n$  as

$$G_n(k) = \begin{cases} 1 & \text{if } A_n(k) = 1 \text{ and } F(k) = 1 \\ 0 & \text{otherwise.} \end{cases} \quad (2)$$

Similarly, the collision event  $C_n(k)$  happens when two or more packets collide with each other and we define  $C_n(k)$  as,

$$C_n(k) = \begin{cases} 1 & \text{if } A_n(k) = 1 \text{ and } F(k) = 0 \\ 0 & \text{otherwise.} \end{cases} \quad (3)$$

The collided packets need to be retransmitted until they are successfully received at the receiver using the proposed collision resolution scheme calculated as in Section III.

Moreover, we assume that each MTD keeps a record of its previous actions, feedback and its current buffer state  $B_n(k)$  up to  $h$  past instants,  $h$  being the *history size*. Hence, at each time slot  $k$ , the tuple

$$S_n(k) = (A_n(k-h), F_n(k-h), A_n(k-h-1), F_n(k-h-1), \dots, A_n(k-1), F_n(k-1), B_n(k)) \quad (4)$$

is referred to as the *local history* or the *state* of device  $n$ , and  $S_H(k) = (S_1(k), \dots, S_N(k))$  is the *global history* of the system.

In this work, we are interested in developing a distributed transmission policy  $\pi(\cdot)$  for slotted RA that can effectively resolve collisions without excess packet delay and also provide

better throughput. We can mathematically define our objective function as

$$\max_{A_n(k)} \sum_{k=1}^K G_n(k) - \rho C_n(k), \forall n \in \mathcal{N}, \quad (5)$$

where  $\rho$  is the weightage given to the collision by device  $n$ . To achieve this objective, we use DQN algorithm with parameter sharing for our multiagent/multiuser environment presented in Section. III.

#### A. Performance Metrics

1) *Throughput*: The average packet success rate or throughput is defined as the number of successfully delivered packets till the total time  $K$ . We define the average throughput as,

$$T = \frac{1}{K} \sum_{k=1}^K \sum_n G_n(k). \quad (6)$$

2) *Packet Collision Rate*: We define the packet collision rate as the number of times collision events happened over time  $K$ . The average collision rate is therefore defined as,

$$Z = \frac{1}{K} \sum_{k=1}^K F(k). \quad (7)$$

3) *Packet Delay*: The delay  $D_n(i)$  of the  $i$ -th packet that has entered the buffer of MTD  $n$ , is defined as the number of time slots between its entrance into the buffer, and its successful transmission. The total number of packets that have been successful transmitted by device  $n$  within  $K$  time slots, is  $\sum_{k=1}^K G_n(k)$ . The sum of delays is equal to

$$\sum_i D_n(i) = \sum_k \mathbb{1}\{B_n(k) > 0\}, \quad (8)$$

where  $\mathbb{1}\{\cdot\}$  is the indicator function. We calculate the average packet delay for device  $n$  after  $K$  time slots as

$$d_n = \frac{\sum_i D_n(i)}{\sum_{k=1}^K G_n(k)}, \quad (9)$$

and the average delay for the whole system is  $\mathcal{D} = \frac{1}{N} \sum_n d_n$

#### B. Baseline Exponential Backoff Policies

We consider EB policies as our baseline schemes with backoff factor of  $\sigma$ . In this paper, we divide EB schemes into non-symmetric EB (nSEB) and symmetric EB (SEB).

1) *Non Symmetric Exponential Backoff Policy*: Let us denote the transmit probability of MTD  $n$  at time slot  $k$  as  $p_n(k)$ . For EB schemes, the transmit probability of the device  $n$  after  $j$  consecutive collisions becomes  $p_n(k) = \sigma^{-j}$ . For non-symmetric EB, if  $i \in \mathcal{N}_c(k)$  where  $\mathcal{N}_c(k) \subseteq \mathcal{N}_a(k)$  is the set of colliding MTDs, then the transmit probability of colliding MTDs  $i \in \mathcal{N}_c(k)$  can be written as,

$$p_i(k) = \begin{cases} \max\left(\frac{p_i(k-1)}{\sigma}, p_{\min}\right) & \text{if collision} \\ p_{\max} & \text{otherwise,} \end{cases} \quad (10)$$

where  $p_{\max}$  and  $p_{\min}$  denote the maximum and minimum transmit probabilities respectively. For  $\sigma = 2$ , the scheme is

referred to as binary nSEB (BnSEB). The Equation (10) shows that the transmit probability is reduced by colliding MTDs only when a collision event occurs. BnSEB is a standard EB scheme that has been used in IEEE 802.11 and IEEE 802.3 standards.

2) *Symmetric Exponential Backoff Policy*: In symmetric EB (SEB), each active MTD increases or decreases its transmission probability  $p_n(k)$  whenever a collision or a no-collision event happens, respectively. Since all devices have the same transmit probability we drop the subscript  $n$  and denote it as  $p(k)$ , which is calculated as

$$p(k) = \begin{cases} \max\left(\frac{p(k-1)}{\sigma}, p_{\min}\right) & \text{if collision} \\ \min(\sigma p(k-1), p_{\max}) & \text{otherwise} \end{cases} \quad (11)$$

For  $\sigma = 2$ , the scheme is referred to as binary SEB (BSEB).

### III. RL ENVIRONMENT AND MULTIAGENT DQN

#### A. RL Environment Formulation

We define our environment as the multi-agent environment with each MTD as an agent<sup>1</sup>, and the physical resource (channel) is shared by all the agents as shown in Fig. 2. The environment is partially observable because each agent  $n$  is unaware of the actions of other agents and it takes its own action  $A_n$  independently based on the observed state  $S_n$ .

1) *State*: We define the *state* of each agent as the local history  $S_n(k)$  observed by the agent at each time slot  $k$ .<sup>2</sup>

2) *Actions*: Similarly, the action of each agent as mentioned above is to transmit  $A_n(k) = 1$ , or to wait  $A_n(k) = 0$ .

The state  $S_n$  of inactive MTDs is masked with zeros and the corresponding action  $A_n$  value is also set to zero.

3) *Reward*: In RL, the goal of an agent in RL is to maximize the long-term expected reward and therefore, the reward function reflects the optimization goal for the environment. Let  $R_n(k) \in \mathbb{R}$  be the *immediate* reward that agent  $n$  obtains at the end of time slot  $k$  after taking the action  $A_n(k)$  and receiving the observation  $F(k)$  from the environment. The accumulated discounted reward for agent  $n$  is defined as

$$\mathcal{R}_n(k) = \sum_{k'=0}^{\infty} \gamma^{k'} R_n(k+k'+1), \quad (12)$$

where  $\gamma \in (0, 1]$  is a discount factor. For our system model, we define the reward  $R_n(k)$  as,

$$R_n(k) = \sum_n G_n(k) - \rho C_n(k), \quad (13)$$

The summation sign in (13) shows that the reward is global, i.e., all MTDs share the same reward, which indicates that the agents are fully cooperative – a common technique to implicitly introduce cooperation among agents in multiagent RL.

<sup>1</sup>We use the terms MTD, device and agent interchangeably in the rest of the paper.

<sup>2</sup>The terms *history* and *state* are used interchangeably in the rest of the paper.

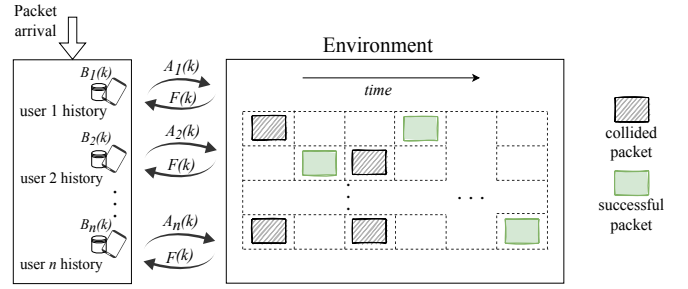


Fig. 2. Interaction of agents/devices with the proposed environment. For each time slot  $k$ , each active device  $n$  takes an action  $A_n(k) \in \mathcal{A}$ , and receives the feedback signal  $F(k)$ . The devices update their buffer state  $B_n(k)$  depending on the feedback signal and the action taken

In our previous work [10], we had employed success only reward  $R_n(k) = \sum_n G_n(k)$  but such reward, as we have observed, is not enough. Due to limited information availability at each agent and partial observability, the algorithm doesn't converge well and the performance degrades as the number of agents grows.

#### B. Multiagent DQN with Parameter Sharing

In Q-learning, Q-values are used to express the expected reward for each state-action pair as

$$Q_n(a, s) = E_{\pi}[\mathcal{R}_n(k) \mid A_n(k) = a, S_n(k) = s] \quad (14)$$

where  $E_{\pi}[\cdot]$  denotes the expectation under the common policy  $\pi$ , with respect to the current state of the agent.

For the DQN [11], a neural network is used to approximate the Q-values  $Q(a, s, \theta) \approx Q^*(s, a)$ , where  $Q(a, s, \theta)$  is the Q-value estimated by the neural network for action  $a$  when the state is  $s$ , and  $\theta$  denotes the weights of the neural network.

In this work, we employ *parameter sharing* method, which basically extends the single agent network to multiple agents [12]. The core idea is to use the same function approximator (e.g., neural network) to calculate the Q-values  $Q_n(a_n, s_n, \theta)$  for all the agents. Parameter sharing allows us to learn a common policy for all the agents in a centralized way, whilst the deployment of the policy for each agent is in a decentralized manner and therefore, we may drop subscript  $n$  from  $Q_n(s, a)$ .

The parameter sharing method proposed in [12] incorporates the IDs of each agent in the state to distinguish between the agents and for each agent to have a unique state every time. In this work, we are employing unsourced RA where new agents can join/leave the network any time. Therefore, we are not using any agent/device IDs in the state to distinguish them. We use the *experience replay* to train the DQN, which is performed by memorizing the experiences of each agent as  $(s(k), a(k), r(k), s(k+1))$  in a replay buffer memory  $\mathcal{D}$  for each iteration. The learning updates are applied on the experience samples  $(s, a, r, s') \sim U(\mathcal{D})$ , that are drawn at random with uniform distribution as mini-batches of size  $M$  from  $\mathcal{D}$ . Moreover, we use two neural networks [13]: The Q-network with parameters  $\theta$  that is used to evaluate and update the actual policy, and the target network with parameters

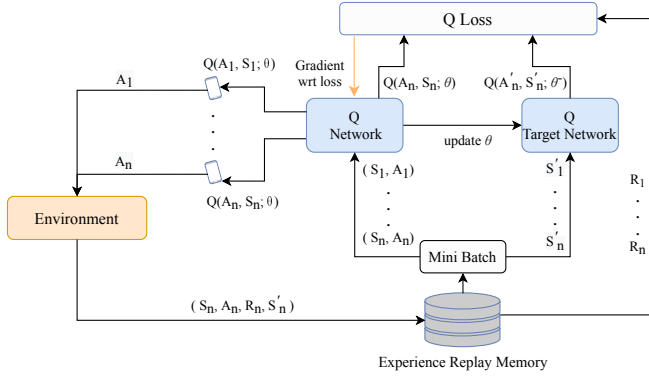


Fig. 3. Schematic of the training of the DQN with parameter sharing

$\theta^-$ . The process is shown in Fig. 3. After each iteration  $i$ , the parameters  $\theta$  are updated minimizing the following loss function,

$$L_i(\theta_i) = \mathbb{E}_{(s,a,r,s') \sim U(\mathcal{D})} \left[ (y_i - Q(a, s; \theta_i)) \right]^2,$$

where  $y_i = r + \gamma \max_{a'} Q(a', s'; \theta_i^-)$  is the target value for the iteration  $i$ .

We obtain the following by differentiating the loss function  $L_i(\theta_i)$  with respect to the weights,

$$\nabla_{\theta_i} L_i(\theta_i) = \mathbb{E}_{(s,a,r,s')} \left[ (y_i - Q(a, s; \theta_i)) \nabla_{\theta_i} Q(a, s; \theta_i) \right]$$

For DQN-RA, at each time slot  $k$ , each MTD  $n$  obtains the observation (feedback)  $F(k)$  after taking the action  $A_n(k) \in \mathcal{A}$ ; it then updates its history  $S_n(k)$  and feeds  $S_n(k)$  to the DQN as input. The output of the DQN the Q-values corresponding to each action. The device  $n$  then follows the policy  $\pi$  by drawing an action  $A_n(k)$  from the following distribution calculated using the softmax policy [14]

$$\pi(a_n | s_n) = \frac{e^{\beta Q(a_n, s_n)}}{\sum_{\tilde{a}_n \in \mathcal{A}} e^{\beta Q(\tilde{a}_n, s_n)}} + \frac{\epsilon}{|\mathcal{A}|}, \quad \forall a_n \in \mathcal{A}, \quad (15)$$

where  $\beta > 0$  is the temperature parameter and  $0 < \epsilon < 1$ , which are used to adjust the balance between *exploration* and *exploitation*.

#### IV. SIMULATION RESULTS AND DISCUSSION

The DQN contain two fully connected hidden layers with 150 and 100 units each. We employ episodic training to produce the results. At the start of each episode, out of  $N$  MTDs, on average  $N_a$  devices become active following the random process, i.e.,  $N_a \sim \text{Poisson}(\lambda_n N)$ . Each MTD  $n \in \mathcal{N}_a$  has one packet in its buffer, i.e,  $B_n(k) = 1 \forall n \in \mathcal{N}_a$ . Each episode comprises of  $K$  time slots and  $K$  depends on the number of MTDs and  $\lambda_n$ . For our results we use  $K = 4\lambda_n N$ , which allows enough time slots for both DQN and EB policies to resolve the collisions and successfully transmit their packets. Since the average arrival rate for each device  $\lambda_n$  remains the same; however due to the fact that the total arrival rate of the system is  $\lambda_n N$ , as the  $N$  grows, the total number of devices becoming active also grow.

#### Algorithm 1: Training of the proposed DQN-RA

---

- 1 **Define**  $\alpha \in (0, 1]$ ,  $\gamma \in [0, 1]$ ,  $\epsilon > 0$  and number of MTDs  $N$
- 2 **Initialize**  $S_n(k) = \mathbf{0}$ ,  $B_n(k) = 0 \forall n \in \mathcal{N}$ , weight update frequency  $L$ ,  $\lambda_n$ , history size  $h$  and total time slots  $K = 4\lambda_n N$
- 3 **for each episode do**
- 4     **Activate**  $N_a$  new MTDs, i.e.,  $N_a \sim \text{Poisson}(\lambda_n N)$   
 $\forall n \in \mathcal{N}$
- 5     **Set**  $B_n(k) = 1 \forall n \in \mathcal{N}_a$
- 6     **for**  $k = 1, \dots, K$  **do**
- 7         **for each MTD**  $n = 1, \dots, N$  **do**
- 8             **if**  $B_n(k) \neq 0$  **then**
- 9                 Observe  $S_n(k)$  as in (4) and feed it to the Q-network
- 10                 Generate the estimate of  $Q(a_n)$   
 $\forall a_n \in \mathcal{A}$
- 11                 Take action  $A_n(k)$  according to (15)
- 12                 Obtain feedback  $F(k)$  as observation and calculate reward  $R_n(k)$
- 13                 Update the buffer  $B_n(k)$  and obtain the next state  $S'_n(k)$
- 14                 Feed  $S'_n(k)$  to both Q-network, and target Q-network
- 15                 Generate estimates from both Q-networks,  $Q(a_n)$  and  $Q_{\text{target}}(a_n)$
- 16             **end**
- 17         **end**
- 18         Train Q-network with minibatch of size  $M$  as input  $S(k) = S_1(k), S_2(k), \dots, S_M(k)$  and output  $M$  Q-values
- 19         **if**  $t\%L = 0$  **then**
- 20             |  $Q_{\text{target}} \leftarrow Q$
- 21         **end**
- 22     **end**
- 23     Reset  $B_n(k) = 0 \forall n \in \mathcal{N}$
- 24 **end**

---

The training and testing process of DQN-RA is depicted in Algorithm. 1 and Algorithm. 2 respectively. The parameters used in the episodic training of the DQN and also to generate the simulation results are given in Table. I. Please note that only devices that are active, i.e.,  $B_n(k) \neq 0$  are passed through the Q-networks. For inactive devices, we use zero-masking where the value of the state is set to 0 values. The states of inactive agents is still used to update the experience replay buffer.

In Fig. 4 we show the reward trends during the training of the DQN for different values of  $N$ . For space constraints, we are not showing for all the values of  $N$  that we have used but they all converge in a similar manner. Small fluctuations are due to the randomness as the number of devices becoming active is not constant or the same for each episode. Next we show the performance of our proposed schemes in terms

---

**Algorithm 2:** Testing phase of the DQN-RA
 

---

```

1 Initialize  $S_n(k) = \mathbf{0}$ ,  $B_n(k) = 0 \forall n \in \mathcal{N}$ ,  $\lambda_n$ , and
   total time slots  $K = 4\lambda_n N$ 
2 Define Number of MTDs  $N$  and history size  $h$ 
3 for each episode do
4   Activate  $N_a$  new MTDs, i.e.,  $N_a \sim \text{Poisson}(\lambda_n N)$ 
    $\forall n \in \mathcal{N}$ 
5   Set  $B_n(k) = 1 \forall n \in \mathcal{N}_a$ 
6   for  $k = 1, \dots, K$  do
7     for each MTD  $n = 1, \dots, N$  do
8       if  $B_n(k) \neq 0$  then
9         Observe  $S_n(k)$  as in (4) and feed it to
          Q-network
10        Generate the estimate of  $Q(a_n)$ 
           $\forall a_n \in \mathcal{A}$ 
11        Take action  $A_n(k)$  according to (15)
12        Obtain feedback  $F(k)$ 
13        Update the buffer  $B_n(k)$  and the next
          state  $S'_n(k)$ 
14      end
15    end
16  end
17  Reset  $B_n(k) = 0 \forall n \in \mathcal{N}$ 
18 end

```

---

TABLE I  
SIMULATION PARAMETERS

Parameter	Value
$\rho$	0.2
$\lambda_n$	0.05
$(p_{\min}, p_{\max})$ for EB schemes	(0.001, 0.9)
Total time slots $K$	$4\lambda_n N$
History size $h$	5
Learning rate	$1e-4$
$(\epsilon, \epsilon_{\min})$	(0.5, 0.1)
Temperature $\beta$	1 – 15
# of hidden layers	2, (150 and 100 units)
Batch size	8
# of episodes (training & testing)	50

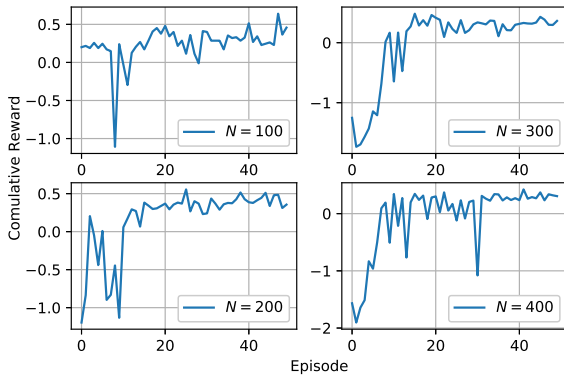


Fig. 4. Average cumulative reward for different values of  $N$ .

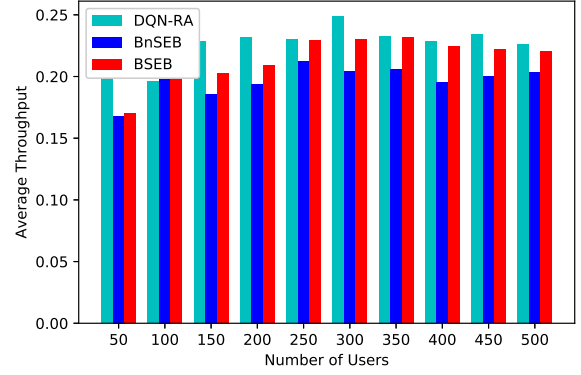


Fig. 5. Average throughput comparison.

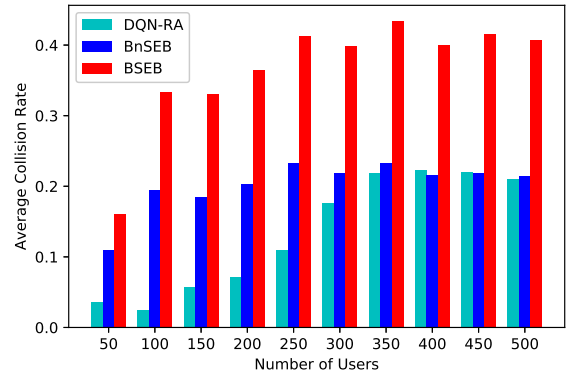


Fig. 6. Average collision rate comparison.

of throughput, delay and collision rate and we compare the performance with binary EB schemes, both BnSEB and BSEB.

The average throughput of the system and the average packet collision rate are shown in Fig. 5 and Fig. 6 respectively. Comparing both Fig. 5 and Fig. 6 it is clear that the learned DQN-RA policy achieves better throughput compared to both BnSEB and BSEB with  $\sigma = 2$  whilst having lower collision rate. Moreover, in Fig. 5, BSEB achieves better throughput as compared to the BnSEB because the devices transmit more aggressively when they increase and decrease their transmit probabilities together and be able to achieve better throughput. However, due to this behavior, BSEB has highest collision rate as compared to the BnSEB as depicted in Fig. 6. Clearly, DQN-RA finds a balance between both approaches and outperforms both BnSEB and BSEB both in terms of average throughput and collision rate. The DQN-RA has similar performance to BnSEB for higher number of MTDs in terms of packet collision rate but it exhibits lower average packet delay even for higher number of devices.

Similarly, Fig. 7 shows the performance of average delay and we can observe that the proposed approach incurs lowest average packet delay as compared to both BnSEB and BSEB as the number of grow. BnSEB has the highest average delay



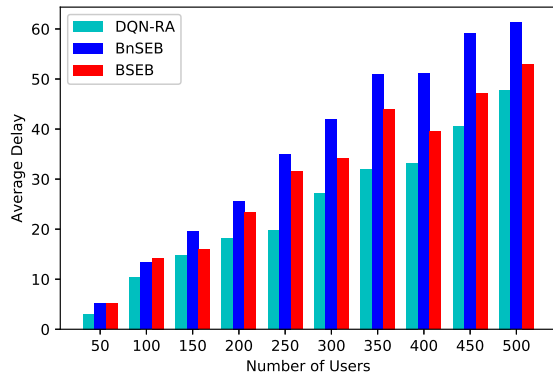


Fig. 7. Average delay comparison.

because packets stay in the buffer due to the fact that devices significantly reduce their transmit probabilities and therefore it is also reflected in the behaviour of this scheme in Fig. 5 which shows that MTDs are unable to transmit frequently even when channel is free and in Fig. 6 it has therefore the low collision rate. It becomes more apparent when the value  $N$  becomes higher. The proposed scheme outperforms both EB techniques even in terms of average packet delay.

We set the history size  $h = 5$  for all the experiments for DQN-RA and the performance for each value of  $N$  is calculated as the average over 50 episodes for all the schemes. We have also tried the experiments with  $h = 1, 3, 10$  but history size  $h = 5$  performs better and increasing  $h$  does not further improve the performance. Due to space constraints we are not showing the results here. Furthermore, the temperature parameter  $\beta$  and  $\epsilon$  are used for exploration and we increase  $\beta$  and decrease  $\epsilon$  during the training for each  $N$ . The  $\epsilon_{\min} = 0.1$ , which is kept at this value to prevent the transmit probabilities (policy) to go to 0 when devices start colliding at the start of each episode. Therefore, the value of  $\epsilon_{\min}$  puts a lower bound on the transmission probability of each MTD for stability.

## V. CONCLUSION

In this work, we propose a collision resolution policy for RA in MTC where the devices can become active and inactive randomly. We provide the performance comparison of our proposed DQN-RA policy with EB schemes and show that our proposed policy performs better in terms of average throughput, collision rate and delay. We use parameter sharing method with DQN to learn a single policy that is learned in a centralized manner and it can be executed distributively by every MTD. We show that our scheme scales well for higher number of MTDs. In our next work, we will use different traffic arrival methods suitable for MTC, e.g., the ones mentioned in [15], and we will explore other multi-agent RL algorithms such as policy gradient methods to learn the transmit probabilities of the devices. Furthermore, for MTC traffic, exploiting the advantages of both scheduled access and

RA might be a better way to manage massive access, which we will also explore in our future work.

## ACKNOWLEDGMENT

The work of A. Pastore and M. Navarro was supported by Grant RTI2018-099722-B-I00 funded by MCIN/AEI/10.13039/501100011033 and by ‘‘ERDF A way of making Europe’’. The work of M. A. Jadoon was supported by the European Union H2020 Research and Innovation Programme through Marie Skłodowska Curie action (MSCA-ITN-ETN 813999 WINDMILL).

## REFERENCES

- [1] C. Bockelmann, N. Pratas, H. Nikopour, K. Au, T. Svensson, C. Stefanovic, P. Popovski, and A. Dekorsy, ‘‘Massive machine-type communications in 5G: physical and MAC-layer solutions,’’ *IEEE Communications Magazine*, vol. 54, no. 9, pp. 59–65, 2016.
- [2] L. Barletta, F. Borgonovo, and I. Filippini, ‘‘The throughput and access delay of slotted-aloha with exponential backoff,’’ *IEEE/ACM Transactions on Networking*, vol. 26, no. 1, pp. 451–464, 2018.
- [3] Y. Chu, S. Kosunalp, P. D. Mitchell, D. Grace, and T. Clarke, ‘‘Application of reinforcement learning to medium access control for wireless sensor networks,’’ *Engineering Applications of Artificial Intelligence*, vol. 46, pp. 23–32, 2015.
- [4] O. Naparstek and K. Cohen, ‘‘Deep multi-user reinforcement learning for distributed dynamic spectrum access,’’ *IEEE Transactions on Wireless Communications*, vol. 18, no. 1, pp. 310–323, 2019.
- [5] C. Zhong, Z. Lu, M. C. Gursoy, and S. Velipasalar, ‘‘Actor-critic deep reinforcement learning for dynamic multichannel access,’’ in *2018 IEEE Global Conference on Signal and Information Processing (GlobalSIP)*, pp. 599–603, 2018.
- [6] S. Wang, H. Liu, P. H. Gomes, and B. Krishnamachari, ‘‘Deep reinforcement learning for dynamic multichannel access in wireless networks,’’ *IEEE Transactions on Cognitive Communications and Networking*, vol. 4, no. 2, pp. 257–265, 2018.
- [7] S. Tomovic and I. Radusinovic, ‘‘A novel deep Q-learning method for dynamic spectrum access,’’ in *2020 28th Telecommunications Forum (TELFOR)*, pp. 1–4, 2020.
- [8] L. de Alfaro, M. Zhang, and J. J. Garcia-Luna-Aceves, ‘‘Approaching fair collision-free channel access with slotted aloha using collaborative policy-based reinforcement learning,’’ in *2020 IFIP Networking Conference (Networking)*, pp. 262–270, 2020.
- [9] H. Yang, Z. Xiong, J. Zhao, D. Niyato, C. Yuen, and R. Deng, ‘‘Deep reinforcement learning based massive access management for ultra-reliable low-latency communications,’’ *IEEE Transactions on Wireless Communications*, vol. 20, no. 5, pp. 2977–2990, 2021.
- [10] M. A. Jadoon, A. Pastore, M. Navarro, and F. Perez-Cruz, ‘‘Deep reinforcement learning for random access in machine-type communication,’’ in *2022 IEEE Wireless Communications and Networking Conference (WCNC)*, 2022.
- [11] Mnih *et al.*, ‘‘Human-level control through deep reinforcement learning,’’ *Nature*, vol. 518, pp. 529–533, Feb. 2015.
- [12] J. K. Gupta, M. Egorov, and M. Kochenderfer, ‘‘Cooperative multi-agent control using deep reinforcement learning,’’ in *Autonomous Agents and Multiagent Systems* (G. Sukthankar and J. A. Rodriguez-Aguilar, eds.), (Cham), pp. 66–83, Springer International Publishing, 2017.
- [13] H. van Hasselt, A. Guez, and D. Silver, ‘‘Deep reinforcement learning with double Q-learning,’’ 2015.
- [14] R. S. Sutton and A. G. Barto, *Reinforcement Learning: An Introduction. (Second Edition)*. Cambridge, MA, USA: A Bradford Book, 2018.
- [15] J. Navarro-Ortiz, P. Romero-Diaz, S. Sendra, P. Ameigeiras, J. J. Ramos-Munoz, and J. M. Lopez-Soler, ‘‘A survey on 5g usage scenarios and traffic models,’’ *IEEE Communications Surveys Tutorials*, vol. 22, no. 2, pp. 905–929, 2020.